

**Appendix I: *O*-GlcNAc Glycosylation Regulates CREB
Activity in Pancreatic Beta Cells**

This work was done in collaboration with Dr. Nathan Lamarre-Vincent.

CREB and *O*-GlcNAc glycosylation have both independently been shown to be critical for beta cell function and dysfunction. Yet little is known about the role of *O*-GlcNAc glycosylation on CREB in beta cell function. Here we show that CREB is highly glycosylated at Ser40 and that CREB glycosylation can be induced by high glucose, glucosamine, and PUGNAc in pancreatic beta cells. We furthermore show that CREB glycosylation represses induced CREB activity on a CRE luciferase construct and on IRS-2, a protein known to be critical for beta cell survival. This data suggests a mechanism wherein hyperglycemia induces CREB glycosylation, which leads to enhanced beta cell death.

Introduction

CREB is a key regulator of both beta cell function and dysfunction. CREB mediates the levels of anti-apoptotic genes *bcl-2* and *IRS-2* in response to prosurvival signals such as GIP and GLP^{1, 2}, and CREB overexpression in cultured beta cell lines protects these cells against cytokine-induced cell death³. Alternatively, suppression of CREB-dependent *IRS-2* gene expression has been implicated in beta cell death¹. Furthermore overexpression of a dominant negative form of CREB in human islets leads to increased apoptosis⁴, and transgenic animals with a beta-cell-specific expression of either a repressive isoform of CREB or a dominant negative form of CREB develop severe diabetes and exhibit decreased beta cell mass^{1,5}.

Previous studies have indicated a role for *O*-GlcNAc in diabetes. Approximately 2–5% of all cellular glucose is metabolized through the hexosamine biosynthesis pathway (HBP) to generate UDP-GlcNAc, and OGT activity is particularly sensitive to UDP-GlcNAc concentrations⁶. *O*-GlcNAc modifies many of the proteins important for insulin

signaling, including IRS-1, IRS-2, and GLUT 4⁷⁻⁹, and increased *O*-GlcNAc levels have been shown to cause insulin resistance in a number of cell types including adipocytes and skeletal muscle^{10, 11}. Studies have also shown that *in vivo* glucosamine (GlcN) injections lead to insulin resistance in normoglycemic rats but not in diabetic rats¹². Furthermore overexpression of OGT *in vivo* in skeletal muscle and fat or in hepatic cells leads to insulin resistance^{13,14} whereas overexpression of OGA in the liver of diabetic mice improves glucose homeostasis¹⁵. Similarly *O*-GlcNAc has been shown to regulate transcription factors important for glucose homeostasis, including FoxO1, NeuroD1, MafA, and PDX-1^{16, 17}.

More recently, flux through the HBP which leads to increased *O*-GlcNAc levels has been shown to contribute to high glucose-induced beta cell death. OGT expression is highest in beta cells, and beta cell *O*-GlcNAc levels respond rapidly to changes in glucose levels *in vivo*¹⁸. OGT and *O*-GlcNAc levels are significantly induced in the islets of diabetic rats as compared to control rats¹⁹. Furthermore, inhibiting glucose flux through the HBP or inhibiting *O*-glycosylation blocks high glucose-induced apoptosis of human islets and cultured rat insulinoma cells⁸. Similarly, blocking the removal of *O*-GlcNAc from proteins in beta cells *in vivo* leads to beta cell death after exposure to high glucose, an affect that is abrogated by inhibiting flux through the HBP¹⁸.

Given the important roles of both CREB and *O*-GlcNAc in beta cell function, we sought to determine how *O*-GlcNAc glycosylation downstream of hyperglycemia may regulate CREB activity.

Results and Discussion

We first sought to determine whether CREB was *O*-GlcNAc glycosylated in pancreatic cells. Pancreases from WT euglycemic rats were isolated and the proteins were chemoenzymatically labeled followed by reaction with aminoxy-PEG to specifically label the *O*-GlcNAc-modified proteins. Although the standard protocol for this technique is to immediately resolve the PEG-labeled lysate by SDS-PAGE, we found that immunoblotting for CREB on such a gel gave numerous background bands, making it difficult to identify the PEG-shifted *O*-GlcNAc-modified CREB population. Thus we immunoprecipitated CREB to better isolate it from the surrounding protein before resolving the sample by SDS-PAGE. Immunoblotting for CREB showed two clear bands, representing nonglycosylated and glycosylated CREB (**Fig. 1a**). From this gel, we could see that CREB is highly glycosylated ($36.5 \pm 4.90\%$) in the pancreas. Furthermore only one PEG-shifted band could be detected for CREB, indicating that CREB is predominantly monoglycosylated in the pancreas. Nevertheless the background antibody signal, near where a second, doubly PEG-shifted CREB signal would reside, makes it difficult to rule out a very low abundant doubly-glycosylated CREB subpopulation such as seen in neurons (see Chapter 5).

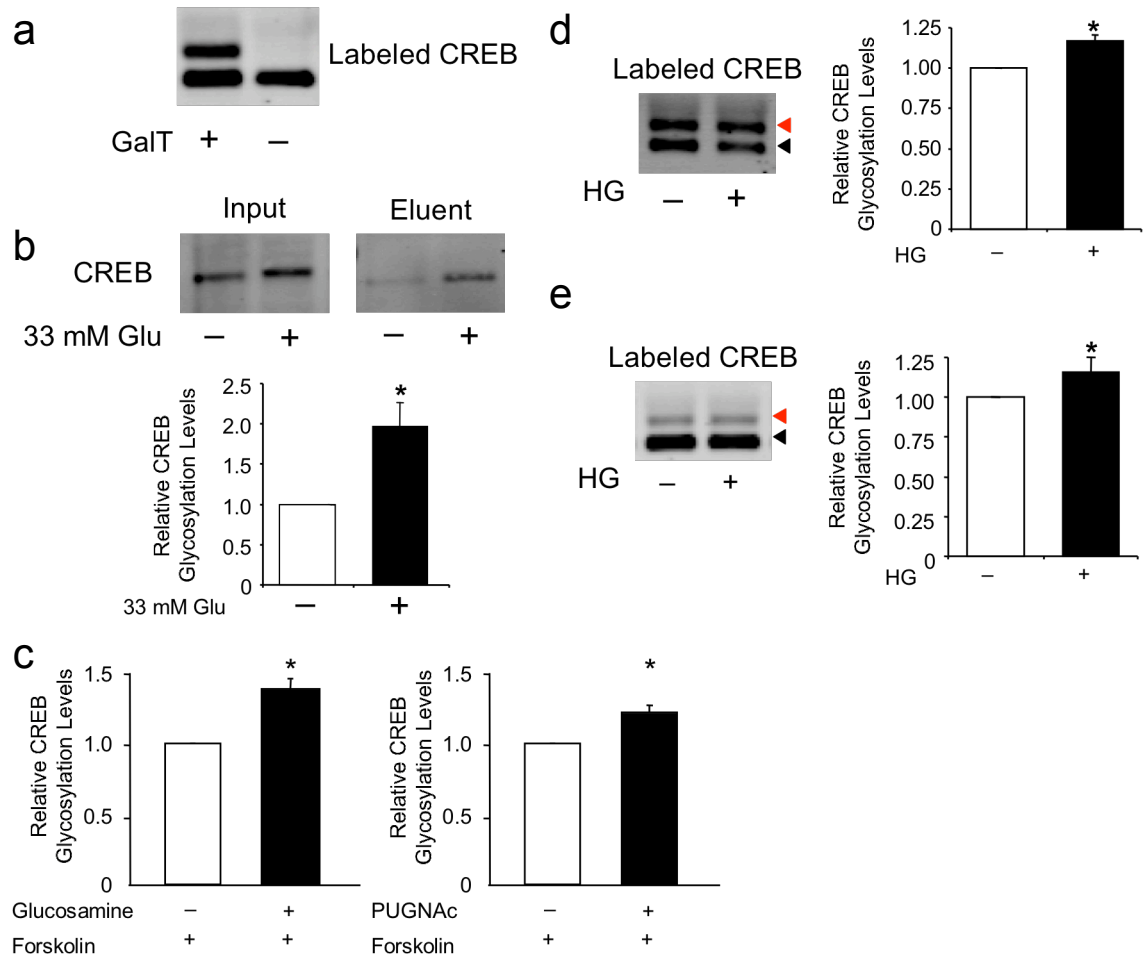


Figure 1: Hyperglycemia induces CREB glycosylation. (a) Rat pancreases were removed and the lysate was chemoenzymatically labeled followed by reaction with aminoxy-PEG and immunoprecipitation of CREB. Eluents were resolved by SDS-PAGE and immunoblotted for CREB. (b) MIN6 cells were cultured in the presence of 5.5 or 33 mM glucose for 96 hours. Cell lysates were chemoenzymatically labeled followed by reaction with aminoxy-biotin and capture by streptavidin. Input and eluent to the streptavidin capture was resolved by SDS-PAGE and immunoblotted for CREB. $n = 3$, * $P < 0.0002$. (c) HIT-T15 cells were treated with GlcN, PUGNAc, or fsk as indicated. Cell lysates were treated as in (b) except that the labeled lysate was immunoprecipitated for CREB. $n = 3$, * $P < 0.01$. (d) Euglycemic and hyperglycemic GK rat pancreases were processed as in (a). $n = 3$, * $P < 0.01$. (e) Euglycemic and hyperglycemic STZ-treated rat pancreases were processed as in (a). $n = 3$, * $P < 0.1$.

General *O*-GlcNAc levels fluctuate with glucose concentration in beta cells, so we wanted to determine whether CREB glycosylation was affected by changes in glucose concentration. We cultured the pancreatic cell line MIN6 in the presence of 5.5 mM or 33 mM glucose for 96 hours and then assayed the levels of *O*-GlcNAc on CREB by

chemoenzymatic labeling followed by biotinylation and streptavidin pulldown (**Fig. 1b**). We found that high glucose induced CREB levels and further induced CREB glycosylation levels. Correcting for the increase in CREB levels, high glucose induced *O*-GlcNAc glycosylation on CREB by 1.97 ± 0.30 -fold compared to low glucose. Previously we have shown that neuronal depolarization induces CREB glycosylation downstream of Ca^{2+} influx (see Chapter 5), and glucose is known to depolarize beta cells leading to Ca^{2+} influx²⁰, so it may be that similar pathways are activated in both cell types. Furthermore, GlcN as well as PUGNAc induced CREB glycosylation in the pancreatic cell line HIT-T15 (**Fig. 1c**). Taken together, this data indicates that *in vitro*, glucose, GlcN, and PUGNAc induce CREB glycosylation levels.

To determine whether hyperglycemia induces CREB glycosylation *in vivo*, we assayed CREB glycosylation levels in a number of different animal models of diabetes, including streptozocin-induced hyperglycemia as well as Goto-Kakizaki (GK) and Zucker Diabetic Fatty (ZDF) rat genetic models of diabetes. In each of these models, the blood glucose level of the experimental, diabetic rats were all over 300 mg / dL compared with control rats, which had blood glucose levels around 100 mg / dL. Again here we PEG labeled the *O*-GlcNAc-modified population of the protein before immunoprecipitating and Western blotting for CREB. We found in the case of the GK and STZ rat models that hyperglycemia induced CREB glycosylation levels $16.9 \pm 0.01\%$ and $15.4 \pm 0.09\%$ respectively (**Fig. 1d, e**). Hyperglycemia did not induce CREB glycosylation in the ZDF rats ($1.03 \pm 0.12\%$). These studies suggest that at least in certain animal models, hyperglycemia is linked to increased CREB glycosylation.

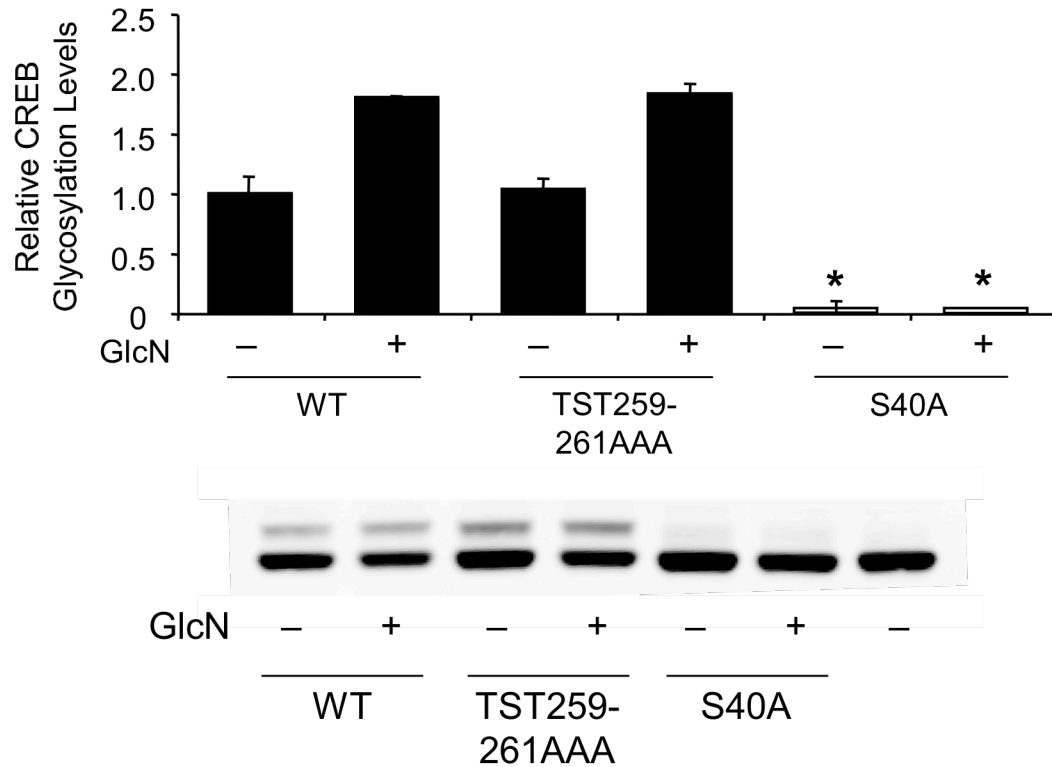


Figure 2: CREB is dynamically glycosylated at Ser40 in HIT-T15 cells. WT, TST259-261AAA, and S40A FLAG-CREB were transfected into HIT-T15 cells and the cells were treated with glucosamine (GlcN) as indicated. Lysates were chemoenzymatically labeled, reacted with aminoxy PEG, and immunoblotted for FLAG. $n = 3$, * $p < 0.01$ compared to WT CREB for each condition.

We have previously identified Ser40 as the major dynamic site of glycosylation in Neuro2A cells and embryonic neurons (see Chapter 5), so we next investigated whether Ser40 glycosylation was also the major dynamic site in beta cells. We transfected HIT-T15 cells with WT, TST259-261AAA, and S40A FLAG-CREB and assayed their glycosylation levels before and after GlcN treatment. The S40A mutant blocked the vast majority ($95 \pm 7\%$) of FLAG-CREB glycosylation while the TST259-261AAA FLAG-CREB mutant had no effect on FLAG-CREB glycosylation levels in HIT-T15 cells (**Fig. 2**). Furthermore, GlcN induced CREB glycosylation on both WT and TST259-261AAA FLAG-CREB ($81\% \pm 14\%$, $83\% \pm 9\%$, respectively) but had no effect on CREB

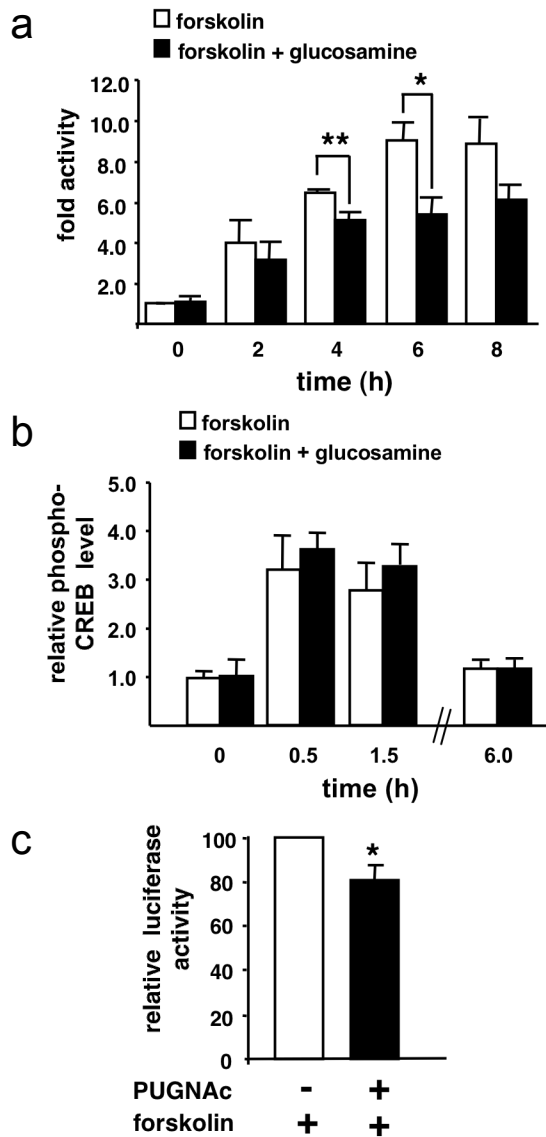


Figure 3: *O*-GlcNAc glycosylation represses CREB transcriptional activity. (a) HIT-T15 cells were transfected with CRE-luciferase and incubated with or without GlcN. Fsk was added to the medium for the times indicated, the harvested cells were lysed, and luciferase activity was quantified. $n = 3-7$, * $P < 0.05$. (b) HIT-T15 cells were incubated with GlcN prior to the addition of Fsk. Cells were harvested and the lysate was analyzed by immunoblotting with an anti-phospho-S133 CREB antibody. (c) Cells were prepared as in (a) except that they were treated with PUGNAc rather than GlcN. $n = 3$, * $P < 0.0005$.

glycosylation of S40A FLAG-CREB ($-0.008\% \pm 0.05\%$), indicating that Ser40 is the only CREB glycosylation site dynamic to GlcN.

Having shown that CREB glycosylation could be dramatically modulated in response to glucose, GlcN, and PUGNAc, we next examined the effect of glycosylation on CREB activity. We transfected HIT-T15 cells with a CRE-luciferase reporter and then tested CREB activity in the presence or absence of GlcN, to enhance CREB glycosylation, or forskolin (fsk), to enhance CREB phosphorylation. Interestingly, we found that GlcN had no effect on CREB activity in non-induced cells, which is different than in

neurons, where removal of glycosylation increased non-induced CREB activity (see Chapter 5). Non-induced nuclear TORC levels differ depending on the cell type²¹, and we have previously shown that CREB glycosylation blocks the interaction with the TORC coactivator (see Chapter 5), so one explanation for this difference could be that the amount of nuclear TORC in HIT-T15 cells is lower than in neurons. Indeed although the absolute amount of TORC in the nucleus was not measured, previous studies have shown that only approximately 15% of non-induced HIT-T15 cells have TORC2 localized to the nucleus²² whereas approximately 40% of TORC1 is localized to the nucleus in non-induced neurons²³. Although glycosylation had little effect on non-induced CREB levels, glycosylation depressed induced CREB activity in a time-dependent manner, reducing CREB activity $39 \pm 10\%$ after 6 hours (**Fig. 3a**). Similar effects were seen following 9 hour PUGNAC treatment (**Fig. 3b**). As seen in neurons, changes in CREB glycosylation had no effect on phospho-Ser133 levels (**Fig. 3c**). This data suggests that induced CREB glycosylation blocks induced CREB activity independent on changes in phospho-Ser133 levels.

CREB has been shown to be critical for regulating *IRS-2* levels that support beta cell survival¹, thus we wanted to know whether CREB glycosylation could effect *IRS-2* mRNA levels in beta cells. Beta cells were treated with GlcN for 9 hours and forskolin for 3 hours. This time GlcN had a significant affect on both non-induced as well as induced levels of *IRS-2* (**Fig. 4a**). To determine whether this could be a direct effect of CREB and OGT on the *IRS-2* promoter, we performed a chromatin immunoprecipitation assay. We found that both CREB and OGT were enriched on the *IRS-2* promoter but not

on the GAPDH promoter (**Fig. 4b**). This indicates that CREB glycosylation may have an important effect on IRS-2 levels.

Taken together, this data suggests a new model for the role of CREB glycosylation in hyperglycemia-induced beta cell death. In this model, hyperglycemia causes increased CREB glycosylation at Ser40. This increased glycosylation leads to decreased IRS-2 levels in both non-induced and induced CREB. These lower IRS-2 levels, then, enhance the susceptibility of beta cells to apoptosis.

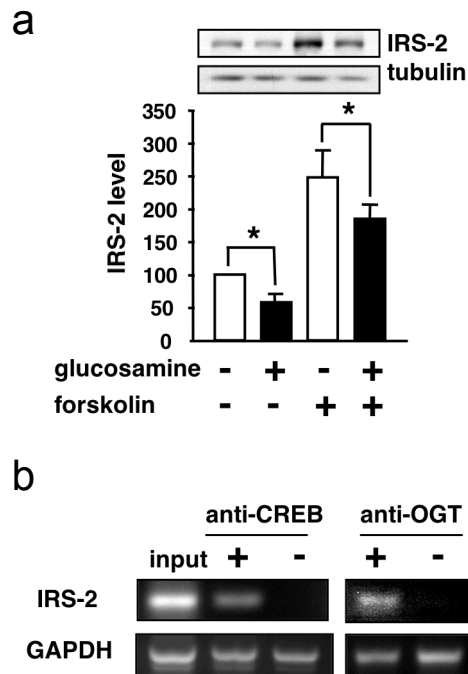


Figure 4: The *IRS-2* gene is a direct target for regulation by CREB and OGT. (a) Cells were treated with or without GlcN. Fsk was added to the medium 3 h after addition of GlcN, and the cells were incubated for an additional 6 h. IRS-2 expression was analyzed by immunoblotting of cell lysates using an anti-IRS-2 antibody and corrected to protein concentration as measured by an anti- α -tubulin antibody. $n = 4$, * $P < 0.03$. (b) Chromatin immunoprecipitation was performed on HIT-T15 cells using antibodies against CREB and OGT. PCR was performed on the IRS-2 or GAPDH promoter.

Methods

Materials. All reagents were purchased from Fisher Scientific unless otherwise specified. RPMI-1640, DMEM, Hank's Buffered Saline Solution (HBSS), fetal bovine serum (FBS) and penicillin/streptomycin were purchased from Invitrogen (Carlsbad, CA). CREB and insulin receptor substrate 2 (IRS-2) antibodies were purchased from Upstate (Charlottesville, VA). OGT and α -tubulin antibodies were purchased from

Sigma-Aldrich (St. Louis, MO). Anti-OGT (AL28) ascites was a generous gift of G.W. Hart (The Johns Hopkins University School of Medicine, Baltimore, MD). *O*-(2-acetamido-2-deoxy-D-glucopyranosylidene)amino-*N*-phenylcarbamate (PUGNAc) was purchased from Toronto Research Chemicals (Toronto, Canada). Forskolin (Fsk) was purchased from Axxora (San Diego, CA), and glucosamine (GlcN) was purchased from Fluka (St. Louis, MO).

Cell Culture. HIT-T15 cells (American Type Culture Collection) were grown in RPMI-1640 supplemented with 10% FBS, 100 U/ml penicillin, 0.1 mg/ml streptomycin (RPMI-1640 complete). Cell passages 66–79 were used for experiments, and cells were subcultured every 6–8 days. MIN6 cells (a generous gift from Dr. Marc Montminy, Salk Institute, La Jolla, CA) were grown in DMEM supplemented with 10% FBS, 100 U/ml penicillin, 0.1mg/ml streptomycin (DMEM complete) and cell passages 25–35 were used for experiments.

Pancreatic Isolation. 150–200 g male Sprague-Dawley rats (Charles River) were euthanized with CO₂ in accordance with IACUC guidelines at the California Institute of Technology. The pancreases were removed and immediately lysed in 2% SDS with 2x protease inhibitor cocktail (Roche) with sonication.

Diabetic Rat Models. Homozygous Goto-Kakizaki rats (11 weeks old) and Wistar Hanover GALAS control rats (11 weeks old) were obtained from Taconic and maintained on a NIH-31 diet formulation (Taconic) and the pancreases were harvested after one

week. Homozygous obese diabetic Zucker diabetic fatty rats (10 weeks old) and heterozygous lean Zucker rats (10 weeks) were obtained from Charles River and the pancreases were harvested after one week. 150–200 g male Sprague-Dawley rats (Charles River) were i.p. injected with 50 mg / kg streptozocin dissolved at 10 mg / mL in 100 mM sodium citrate, pH 4.5. The pancreases were harvested after 72 hours.

Plasmids. pFC6a-CREB, pFC6a-CREB(AAA), pFC6a-CREB(S40A) were generated by subcloning wild-type CREB, TST259-261AAA, and S40A mutant CREB from the respective pET23b+ vectors into the pFLAG-CMV-6a *E. coli* and mammalian expression vector (Sigma-Aldrich) using primers with 5' EcoRI and 3' BamHI restriction sites.

Drug Treatments. GlcN and Fsk treatments were performed as follows. HIT-T15 and MIN-6 cells were used at 50–75% confluence. Cells were pretreated with RPMI-1640 complete (HIT-T15 cells) or DMEM complete (MIN6 cells) supplemented with 10 mM GlcN in 2 mM HEPES, pH 7.5 for 3–12 h as indicated before treatment with the appropriate media supplemented with 10 mM Fsk or vehicle (DMSO) with or without 10 mM GlcN in 2 mM HEPES, pH 7.5 for indicated times.

PUGNAC treatments were performed as follows. Cells were pretreated for 3–12 h as indicated with the appropriate media supplemented with 100 mM PUGNAC before the addition of 10 mM Fsk for indicated times.

Chemoenzymatic Labeling and Detection of O-GlcNAc Glycosylation.

Chemoenzymatic and PEG labeling was performed as previously described (see Chapter

5) except that 2X Complete™ (Roche) and 2X Halt™ (Pierce) protease inhibitors were added at each step. CREB was immunoprecipitated from the PEG reaction as described below. Chemoenzymatic and biotin labeling followed by streptavidin capture and elution was performed as previously described (see Chapter 2). Chemoenzymatic and biotin labeling followed by CREB immunoprecipitation is described here: After drug treatment, cells were harvested and the cell pellet was lysed in boiling lysis buffer (1% SDS supplemented with protease inhibitors (Complete Protease Inhibitor Cocktail Tablets, Roche, Indianapolis, IN), sonicated for 5 s, and boiled for 8 min. After centrifugation at 21,500 x g for 5 min, the supernatant was collected, and the protein concentration was measured using the BCA assay (Pierce, Rockford, IL). One volume of denatured cell extract was diluted into four volumes of dilution buffer (10 mM HEPES pH 7.9, 1.8% Triton X-100, 100 mM NaCl, 10 mM MnCl₂, containing protease inhibitors (5 mg/ml pepstatin, 5 mg/ml chymostatin, 20 mg/ml leupeptin, 20 mg/ml aprotinin and 20 mg/ml antipain) and 1 mM phenylmethylsulfonyl fluoride (PMSF). Diluted extract was then supplemented with 1.25 mM adenosine 5'-diphosphate, 0.5 mM analogue **1** and 20 µg/mL mutant Y289L GalT (64). Control reactions were prepared lacking enzyme or analogue **1** to measure any nonspecific reactivity of streptavidin-HRP (see **Fig. 1**). The reaction mixture was incubated at ~5–7° C for 10–12 h, and dialyzed into 10 mM HEPES, pH 7.9 containing 5 M urea at ~5–7° C (3 x 3 h). Following dialysis the sample was acidified to pH 4.8 by adding NaOAc pH 3.9 (50 mM final concentration). The reaction was initiated with the addition of *N*-(aminoxycetyl)-*N'*-(D-biotinoyl) hydrazine (2.5 mM final concentration, Dojindo, Gaithersburg, MD) and incubated at room temperature for 16–20 h, the sample was then dialyzed into CREB immunoprecipitation

(IP) buffer (10 mM HEPES pH 7.9, 100 mM KCl, .2% Triton X-100 and 1mM EDTA) (1x overnight and 2 x 2 h). After dialysis, the sample was centrifuged for 5 min at 21,500 x g, and protein concentration was measured. Lysate was supplemented with protease inhibitors (5 mg/ml pepstatin, 5 mg/ml chymostatin, 20 mg/ml leupeptin, 20 mg/ml aprotinin, and 20 mg/ml antipain) and volumes were normalized such that equivalent amounts and concentrations of lysate were used for immunoprecipitation. Lysate was first precleared for 1 h at $\sim 5-7^{\circ}$ C with protein A sepharose and the supernatant was incubated with rabbit anti-CREB antibody (Upstate) for 3-4 h at $\sim 5-7^{\circ}$ C. Protein A sepharose was then added and incubated with the lysate for 1 h at $\sim 5-7^{\circ}$ C. The supernatant was collected as flowthrough, and the protein A sepharose was washed with CREB IP buffer (3 X), PBS (3 X) and 50 mM Na_2HPO_4 (1 X). The immunoprecipitated protein was eluted using SDS-PAGE loading buffer, resolved by SDS-PAGE, and analyzed by Western blotting.

Luciferase Assay. HIT-T15 cells transfected using Targefect F2 transfection reagent (3 mg/ml, Targeting Systems, Santee CA) following the manufacturers instructions. Briefly, HIT-T15 cells were grown to $\sim 75\%$ confluence in 60 mm dishes. In studies of endogenous CREB activity, cells were co-transfected with 1 $\mu\text{g}/\text{ml}$ pCRE-Luc (Stratagene) and 0.5 $\mu\text{g}/\text{ml}$ pSV- βGal using the Targefect F2 transfection reagent. In control Gal4 reactions, cells were co-transfected with 1 $\mu\text{g}/\text{ml}$ pFR-Luc (Stratagene), 0.5 $\mu\text{g}/\text{ml}$ pcDNA3.1-Gal4, and 0.5 $\mu\text{g}/\text{ml}$ pSV- βGal . Cells were treated with Fsk/GlcN or Fsk/PUGNAc ~ 24 h post-transfection.

Harvested cells were lysed in 1 x Reporter Lysis Buffer (Promega) with brief sonication on ice. Samples were centrifuged for 5 min at 21,000 x g. Supernatant was used for the measurement of luciferase and β -galactosidase and Western blot analysis. Luciferase activity was measured using Bright-GloTM luciferase assay system (Promega) on an Opticom 1 luminometer (MGM instruments, Hamden, CT). Luciferase activity and transfection efficiency were corrected by measurement of β -galactosidase activity.

Western Blotting Analysis. Total cell lysates were prepared by cell lysis in boiling 1% SDS with protease (5 μ g/ml pepstatin, 5 μ g/ml chymostatin, 20 μ g/ml leupeptin, 20 μ g/ml aprotinin and 20 μ g/ml antipain) and phosphatase inhibitors (20 mM NaF, 1 mM Na₃VO₄, 0.05 mM Na₂MO₄) by sonication. Samples were resolved by 10% SDS-PAGE or by 4–12% Bis-Tris PAGE and transferred to nitrocellulose. The following antibodies were used for Western blot analysis: anti-CREB antibody (1 μ g/ml), anti-phospho-CREB(Ser133) antibody (1 μ g/ml), anti-IRS-2 antibody (1 μ g/ml), and anti-OGT (1 μ g/ml), anti- α -tubulin (0.2 μ g/ml). Blots were visualized by chemiluminescence (Supersignal West Pico, Pierce) on Hyperfilm ECL chemiluminescent film (GE Healthcare Bio-Sciences). Relative band intensity was quantified by analysis of scanned images using NIH Image 1.52 software.

Chromatin Immunoprecipitation (ChIP). ChIP was performed as previously described (see Chapter 5). The following primers were used. IRS-2 (NM_001081212) primers 5'-CCCGCCAGCACTCGCTC-3' and 5'-CGGACGTCATCAGAGCC-3' amplify a 174 bp product corresponding to bp -343 to -169.

RNA isolation and RT-PCR. HIT-T15 cells were grown in 60 mm dishes to a confluence of 50–75% ($\sim 5\text{--}7 \times 10^5$ cells). Cells were pretreated with either RPMI-1640 complete supplemented with 10 mM GlcN in 2 mM HEPES pH 7.5 or RPMI-1640 complete for 3 h before treatment with RPMI-1640 complete supplemented with 10 μ M Fsk and 10 mM GlcN in 2 mM HEPES pH 7.5 or 10 μ M Fsk for 1 h, respectively.

RNA was isolated using Qiagen RNeasy mini-columns following the manufacturer's procedure for the isolation of cytoplasmic RNA from animal cells (Qiagen). cDNA was prepared using oligo dT₁₂₋₁₈ primers (Invitrogen) and Transcriptor reverse transcriptase (Roche). IRS-2 (NM_001081212) primers 5'-GAGCATGGATAGACCCTGA-3' and 5'-GCAGAGGCGACCTGAACTAC-3' amplify a 211 bp product corresponding to bp +1617 to +1817. Mouse β -actin (NM_007393.3) primers 5'-TGTTACCAACTGGGACGACA-3' and 5'-GGGGTGTGAAGGTCTCAA-3' amplify a 165 bp product corresponding to bp +225 to +390. Samples were analyzed with 25–38 cycles of semi-quantitative PCR using Taq PCR_X DNA polymerase (Invitrogen). PCR products were loaded onto 2% agarose/ethidium bromide gels and visualized on an AlphaImager 3400 (Alpha Innotech Corp., San Leandro CA). Band intensity was quantified using software AlphaEaseFC software version 4.0.1 (Alpha Innotech Corp.).

Statistical Analysis. All experiments were repeated a minimum of three times. Results are presented as the mean value \pm one standard error of the mean (SEM). Statistical significance was calculated using the Student's T-test.

References

1. Jhala, U.S. *et al.* cAMP promotes pancreatic beta-cell survival via CREB-mediated induction of IRS2. *Genes Dev* **17**, 1575-1580 (2003).
2. Kim, S.-J., Nian, C., Widenmaier, S. & McIntosh, C.H.S. Glucose-dependent insulinotropic polypeptide-mediated up-regulation of beta-cell antiapoptotic Bcl-2 gene expression is coordinated by cyclic AMP (cAMP) response element binding protein (CREB) and cAMP-responsive CREB coactivator 2. *Mol Cell Biol* **28**, 1644-1656 (2008).
3. Jambal, P. *et al.* Cytokine-mediated down-regulation of the transcription factor cAMP-response element-binding protein in pancreatic beta-cells. *J Biol Chem* **278**, 23055-23065 (2003).
4. Sarkar, S.A. *et al.* Dominant negative mutant forms of the cAMP response element binding protein induce apoptosis and decrease the anti-apoptotic action of growth factors in human islets. *Diabetologia* **50**, 1649-1659 (2007).
5. Inada, A. *et al.* Overexpression of inducible cyclic AMP early repressor inhibits transactivation of genes and cell proliferation in pancreatic beta cells. *Mol Cell Biol* **24**, 2831-2841 (2004).
6. Hart, G.W., Housley, M.P. & Slawson, C. Cycling of O-linked beta-N-acetylglucosamine on nucleocytoplasmic proteins. *Nature* **446**, 1017-1022 (2007).
7. Ball, L.E., Berkaw, M.N. & Buse, M.G. Identification of the major site of O-linked beta-N-acetylglucosamine modification in the C terminus of insulin receptor substrate-1. *Mol Cell Proteomics* **5**, 313-323 (2006).
8. D'Alessandris, C. *et al.* Increased O-glycosylation of insulin signaling proteins results in their impaired activation and enhanced susceptibility to apoptosis in pancreatic beta-cells. *FASEB J* **18**, 959-961 (2004).
9. Buse, M.G., Robinson, K.A., Marshall, B.A., Hresko, R.C. & Mueckler, M.M. Enhanced O-GlcNAc protein modification is associated with insulin resistance in GLUT1-overexpressing muscles. *Am J Physiol Endocrinol Metab* **283**, E241-250 (2002).
10. Teo, C.F., Wollaston-Hayden, E.E. & Wells, L. Hexosamine flux, the O-GlcNAc modification, and the development of insulin resistance in adipocytes. *Mol Cell Endocrinol* **318**, 44-53 (2010).
11. Arias, E.B., Kim, J. & Cartee, G.D. Prolonged incubation in PUGNAc results in increased protein O-Linked glycosylation and insulin resistance in rat skeletal muscle. *Diabetes* **53**, 921-930 (2004).
12. Rossetti, L., Hawkins, M., Chen, W., Gindi, J. & Barzilai, N. In vivo glucosamine infusion induces insulin resistance in normoglycemic but not in hyperglycemic conscious rats. *J Clin Invest* **96**, 132-140 (1995).
13. McClain, D.A. *et al.* Altered glycan-dependent signaling induces insulin resistance and hyperleptinemia. *Proc Natl Acad Sci USA* **99**, 10695-10699 (2002).

14. Yang, X. *et al.* Phosphoinositide signalling links O-GlcNAc transferase to insulin resistance. *Nature* **451**, 964-969 (2008).
15. Dentin, R., Hedrick, S., Xie, J., Yates, J. & Montminy, M. Hepatic glucose sensing via the CREB coactivator CRTC2. *Science* **319**, 1402-1405 (2008).
16. Issad, T. & Kuo, M. O-GlcNAc modification of transcription factors, glucose sensing and glucotoxicity. *Trends Endocrinol Metab* **19**, 380-389 (2008).
17. Vanderford, N.L., Andrali, S.S. & Ozcan, S. Glucose induces MafA expression in pancreatic beta cell lines via the hexosamine biosynthetic pathway. *J Biol Chem* **282**, 1577-1584 (2007).
18. Liu, K., Paterson, A.J., Chin, E. & Kudlow, J.E. Glucose stimulates protein modification by O-linked GlcNAc in pancreatic beta cells: linkage of O-linked GlcNAc to beta cell death. *Proc Natl Acad Sci USA* **97**, 2820-2825 (2000).
19. Akimoto, Y., Kreppel, L.K., Hirano, H. & Hart, G.W. Increased O-GlcNAc transferase in pancreas of rats with streptozotocin-induced diabetes. *Diabetologia* **43**, 1239-1247 (2000).
20. Henquin, J.C. Triggering and amplifying pathways of regulation of insulin secretion by glucose. *Diabetes* **49**, 1751-1760 (2000).
21. Bittinger, M.A. *et al.* Activation of cAMP response element-mediated gene expression by regulated nuclear transport of TORC proteins. *Curr Biol* **14**, 2156-2161 (2004).
22. Jansson, D. *et al.* Glucose controls CREB activity in islet cells via regulated phosphorylation of TORC2. *Proc Natl Acad Sci USA* **105**, 10161-10166 (2008).
23. Li, S., Zhang, C., Takemori, H., Zhou, Y. & Xiong, Z.-Q. TORC1 regulates activity-dependent CREB-target gene transcription and dendritic growth of developing cortical neurons. *J Neurosci* **29**, 2334-2343 (2009).